

RESEARCH ARTICLE

Complementary responses of morphology and physiology enhance the stand-scale production of a model invasive species under elevated CO₂ and nitrogen

Thomas J. Mozdzer^{1,2†} | Joshua S. Caplan^{1,2†} ¹Department of Biology, Bryn Mawr College, Bryn Mawr, Pennsylvania²Smithsonian Environmental Research Center, Edgewater, Maryland**Correspondence**Thomas J. Mozdzer
Email: tmozdzer@brynmawr.edu**Present address**

Joshua S. Caplan, Department of Landscape Architecture & Horticulture, Temple University, Ambler, Pennsylvania

Funding information

Maryland Sea Grant, University of Maryland, Grant/Award Number: SA7528082 and SA7528114-WW; National Science Foundation, Grant/Award Number: DEB-0950080, DEB-1457100 and DEB-1557009; Bryn Mawr College; Smithsonian Institution

Handling Editor: Janne Alahuhta

Abstract

1. Elevated atmospheric carbon dioxide (eCO₂) concentrations and nitrogen (N) enrichment are known to enhance plant productivity and invasion. However, the implications of their interactive effects for plant productivity are not well understood, especially at the stand scale, presumably because morphological and physiological responses to these global change factors are rarely studied together in the field or assessed at the stand level.
2. We first determined how leaf-level morphological and physiological traits responded to factorial combinations of ambient and elevated CO₂ and N. We collected trait data from the model invasive species *Phragmites australis* (common reed) that were measured over 3 years in a long-term global change field experiment. We then combined the trait data and additional descriptions of *P. australis* canopies in a simulation model of carbon assimilation to determine how morphology and physiology contribute to *P. australis*' stand-scale productivity.
3. At the leaf level, we found that light-saturated rates of photosynthesis were strongly stimulated by eCO₂ (37%) and that this effect was enhanced by increasing salinity. N had a smaller effect (17% stimulation) on physiological responses than eCO₂, but leaf morphological traits responded primarily to N; plant height increased by 27% and leaf area increased by 47%.
4. Stand-scale simulations demonstrated that that morphological and physiological adjustments induced approximately additive responses when *P. australis* experienced both eCO₂ and N enrichment. The simulations also indicated that morphological changes (which were primarily associated with canopy size) influenced stand-scale carbon assimilation more than physiological changes. Moreover, 97% of the N response was due to changes in morphology, whereas 62% of the eCO₂ response was caused by physiological shifts.
5. Our analysis indicates that morphological and physiological trait responses to elevated CO₂ and nitrogen are likely to enhance the productivity of *P. australis* in complementary ways, potentially accelerating its invasion in North America. Furthermore, our data suggest that changes in morphological traits may have a greater influence on carbon gain than leaf-level physiology under near-future

[†]These authors contributed equally to this work.

environmental conditions. Our study also highlights the importance of accounting for both morphological and physiological responses when attempting to infer global change responses from leaf-level data.

KEYWORDS

carbon dioxide, functional traits, global change, leaf morphology, nitrogen eutrophication, photosynthesis, *Phragmites australis* (common reed)

1 | INTRODUCTION

Relatively little attention has been given to invasive plant responses to global change factors in a field setting, even though invasive species may have disproportionately large effects on ecosystems they invade. There is substantial evidence that global-scale environmental changes, such as rising atmospheric carbon dioxide (CO₂) concentrations and anthropogenic nitrogen (N) enrichment, can enhance the expansion of invasive, non-native plant species (Bradley, Blumenthal, Wilcove, & Ziska, 2010; Gonzalez et al., 2010; Richards, Bossdorf, Muth, Gurevitch, & Pigliucci, 2006). However, many studies of invasive plant responses to global change are based on short-term experiments in containerized or common garden settings. While these experiments have yielded many valuable insights, their results do not necessarily represent plant responses under field conditions. For example, they vastly simplify the community context (Dukes, 2000), are subject to pot limitation (Thomas & Strain, 1991), and rarely account for interacting environmental factors (Richards et al., 2006). They also overestimate growth responses (Poorter et al., 2016) and are unable to account for the effects of natural climatic variation on functional trait expression (Hulme, 2008). Furthermore, many studies typically identify one or a few functional traits that are highly responsive to global change factors and speculate how changes in those traits may facilitate invasion without empirically evaluating longer-term or larger-scale effects (e.g. Caplan, Wheaton, & Mozdzer, 2014; Sullivan, Wildova, Goldberg, & Vogel, 2010). Moreover, short-term, containerized studies only modestly predict field-scale responses (Poorter et al., 2016). We lack long-term studies of both invasive and non-invasive species that examine how morphological and physiological traits shift at leaf and larger scales to shape plant phenotype, especially in the context of global change.

Regardless of origin (native vs. introduced) or aggressiveness (invasive vs. non-invasive), elevated CO₂ (eCO₂) concentrations are generally predicted to increase physiological performance in C₃ plants. Typically, growth under eCO₂ increases light-saturated photosynthetic rates (A_{sat}), increases instantaneous water use efficiency (WUE_i), decreases stomatal conductance (g_s), and concomitantly decreases stomatal size and/or density (Ainsworth & Long, 2005 and citations within). Additionally, in the case of halophytes, many of the negative effects of salinity are reduced under eCO₂, at least within moderate salinity ranges (Ball & Munns, 1992). In many cases, invasive species (reviewed in Bradley et al., 2010), or even invasive genetic lineages within species (Mozdzer & Megonigal, 2012),

exhibit more strongly enhanced productivity under eCO₂ than do non-invasive plant species or conspecific lineages. Given these physiological enhancements, it is likely that eCO₂ will promote the invasion of numerous C₃ plants in the coming century.

Nitrogen (N) enrichment is also well known to promote plant productivity and invasion (Gonzalez et al., 2010). The particularly strong response of some invasive plant species to N has been associated with greater phenotypic plasticity compared to non-invasive congeners, resulting in greater productivity, tissue N content, chlorophyll concentration and photosynthetic rates, ultimately manifesting in enhanced growth and spread (Davidson, Jennions, & Nicotra, 2011; Mozdzer et al., 2012; Richards et al., 2006).

While considerable information exists on the direct effects of global change on plant traits spanning biochemical to leaf scales, surprisingly little is known about how morphological and physiological functional trait responses combine under interacting global change factors, particularly in a field setting. It is clear that elevated CO₂ concentrations induce physiological changes that may enhance growth rates and that these changes stimulate stand-scale productivity (Ainsworth & Long 2005; Temme, Liu, Cornwell, Cornelissen, & Aerts, 2015). However, leaf-level physiological enhancements may not translate into stand-scale enhancements (reviewed by Way, Oren, & Kroner, 2015), highlighting the value of multifactor elevated CO₂ experiments. While N enrichment typically increases plant growth (see above), enhancements in gross primary productivity (GPP) have also been associated with changes in leaf area index (LAI; Hikosaka et al., 2016). Global change studies that combine these two factors have the potential to uncover inhibitory and synergistic effects that can scale up to affect ecosystem processes such as GPP.

Given its cosmopolitan distribution, high genetic variation and high phenotypic plasticity, *Phragmites australis* (Cav.) Trin. ex. Stued. (common reed) is considered by some to be a model organism for addressing questions in invasion ecology and plant functional responses to global change (Eller et al., 2017; Meyerson, Cronin, & Pysek, 2016; Packer et al., 2017). Although there are native lineages of the species in North America, a Eurasian lineage (haplotype M) was introduced in the 1800s and has become one of the most ubiquitous invasive species in wetland ecosystems across the continent (Chambers, Meyerson, & Saltonstall, 1999). As a C₃ facultative halophyte, it invades freshwater, brackish and saline wetlands, but its distribution is thought to be limited by high salinity (Chambers, Osgood, Bart, & Montalto, 2003; Mozdzer, Brisson, & Hazelton, 2013). Because it has responded strongly to eCO₂ and N in containerized experimental

conditions (Caplan et al., 2014; Eller, Lambertini, Nguyen, & Brix, 2014; Mozdzer & Megonigal 2012) and is among the most well-studied organisms globally (Meyerson et al., 2016), it is an appropriate species for investigating C_3 plant responses to the interactive effects of eCO_2 and N on plant functional traits.

Using data collected over 3 years from an open-top chamber field experiment, we evaluated the effects of elevated CO_2 and N eutrophication on leaf-level physiological and morphological traits of *P. australis*. Temporal variation in tidewater salinity through the period of study also allowed us to evaluate the influence of salinity on photosynthetic responses to these global change factors. Finally, using a simulation model of stand-scale carbon assimilation, we integrated the trait data with other descriptors of *P. australis* canopies to evaluate the composite effects of its morphological and physiological responses to elevated CO_2 and N enrichment.

2 | MATERIALS AND METHODS

2.1 | Field experiment

This study was conducted at the Smithsonian Institution's Global Change Research Wetland (GCREW; 38.8742°N, 76.5474°W), which is brackish tidal marsh located in the Rhode River subestuary of the Chesapeake Bay. Soils at this site are predominantly organic (>80%) to 5 m depth. The marsh has a mean tidal range of 44 cm and a mean salinity of 10 ppt (range = 3–15 ppt). An introduced lineage of *P. australis* (haplotype M) began establishing in the marsh around 1970 (McCormick, Kettenring, Baron, & Whigham, 2010). The native community is dominated by the C_3 sedge *Schoenoplectus americanus* and the C_4 grasses *Spartina patens* and *Distichlis spicata*.

Twelve open-top chambers (1.25 × 2.5 × 4.4 m, W × L × H) were established at the interface of an expanding *P. australis* stand and the adjacent high-marsh community in 2010. Before treatments were applied, each chamber contained 19.7 ± 2.1 ($M \pm SD$) *P. australis* stems, with no significant differences among treatments. Within each of three blocks, chambers were randomly assigned a CO_2 level (ambient or elevated by ~300 ppmv) and a nitrogen level (ambient or +25 g N m² year⁻¹). Our elevated CO_2 level represents conditions expected at the end of the century under moderate CO_2 emissions scenarios (e.g. RCP6; Meinshausen et al., 2011) and our level of N addition is a typical N loading rate for an estuary of a eutrophied watershed (Hopkinson & Giblin, 2008); both have been used in other long-term experiments in native plant communities at GCREW (Drake, 2014; Langley, Mckee, Cahoon, Cherry, & Megonigal, 2009). Treatments were applied factorially, such that the four possible treatment combinations occurred in each block. Chambers with elevated CO_2 were fumigated from May through November each year, beginning in 2011; chamber walls were removed for the remaining months of each year. Ambient air was amended with pure CO_2 to reach a diurnally varying target concentration; the target was determined from samples of ambient air drawn in sequence from each chamber and measured using an infrared gas analyser

(LI-6262, LI-COR Biosciences, Lincoln, Nebraska). Ambient chambers were fumigated with unamended air. Further details on chamber design and CO_2 regulation are described elsewhere (Caplan, Hager, Megonigal, & Mozdzer, 2015; Drake, Leadley, Arp, Nassiry, & Curtis, 1989). Beginning in 2011, N-treated chambers were fertilized with ammonium chloride monthly from May through September (5 g N m⁻² month⁻¹) using a backpack sprayer. Ammonium was applied as it is the dominant form of dissolved inorganic nitrogen at the site; it occurs at levels ranging from 10 to 400 $\mu\text{mol N L}^{-1}$ at 10 cm soil depth, while nitrate is undetectable (Keller, Wolf, Weisenhorn, Drake, & Megonigal, 2009).

2.2 | Trait measurements

Leaf-level physiological parameters were determined from photosynthetic light response curves measured monthly on up to four (but typically three) haphazardly selected plants per chamber ($n = 279$ total curves). Measurements took place in June, July and August from 2011 to 2013 using LI-6400s (LI-COR Biosciences, Lincoln, Nebraska). We measured the photosynthetic response of the 3rd or 4th fully emerged leaf on each plant while they were exposed to a sequence of nine light levels (2,000, 1,500, 1,000, 700, 400, 200, 50, 25, 0 $\mu\text{mol photons m}^{-2} \text{s}^{-1}$). Target block temperatures approximated the ambient air temperature (30°C) while reference CO_2 concentrations approximated those of the open-top chambers (400 or 700 ppmv). Measurements were taken between the hours of 10:00 and 15:00. Data on net photosynthesis (A_{net}) were fit with a non-rectangular hyperbolic function (Prioul & Chartier, 1977) using nonlinear regression (nls function in R):

$$A_{\text{net}} = \frac{\varphi\text{PPFD} + A_{\text{sat}} - \sqrt{(\varphi\text{PPFD} + A_{\text{sat}})^2 - 4k\varphi A_{\text{sat}}\text{PPFD}}}{2k} - R_d$$

Curve fitting yielded values for the following parameters: quantum efficiency (φ), light-saturated CO_2 assimilation rate (A_{sat}), convexity (k) and dark respiration rate (R_d).

To evaluate the effects of salinity on leaf-level carbon assimilation, we calculated the mean salinity (from 15-min interval data) of water in the Rhode River on days that gas exchange measurements took place. Salinity was measured with a YSI 6600 sonde located 1.4 km downstream of the study site in the same subestuary. The site receives the same flood water that is measured by the sonde and freshwater discharge into the tidal creek and marsh is known to be negligible (Jordan & Correll, 1985). Therefore, it is reasonable to assume that the salinity of the tide water remained highly correlated with water column salinity 1.4 km downstream during our measurement period.

We measured the heights of all *P. australis* stems in chambers at the time of peak biomass and maximum canopy development (late July to early August) in 2011, 2012 and 2013 ($n = 2,396$ stems). In 2011, we also collected the 3rd or 4th fully expanded leaf from each *P. australis* stem in the experiment ($n = 604$ leaves). Areas and dry masses of these leaves were measured subsequently and

used to calculate specific leaf area (SLA), that is, leaf area per unit mass. In mid-July 2013, we measured the width and length of all leaves on three haphazardly selected stems per chamber ($n = 282$ leaves). All leaf scans were made in situ using an LI-3100C portable leaf area metre (LI-COR Biosciences, Lincoln, Nebraska). As a metric of narrowness, we calculated the ratio of the width of each leaf (measured at its widest point) to its length. An index of leaf chlorophyll concentration (*CCI*) was measured in July 2013 on one leaf from each of 12–15 randomly chosen stems within each chamber ($n = 171$ leaves). We used a CCM-200 chlorophyll content metre (Opti-Sciences, Hudson, New Hampshire) for these measurements.

In September 2013, we haphazardly collected three leaves from each chamber for stomatal measurements. Epidermal peels were taken of the abaxial and adaxial surfaces across the broadest section of each leaf using clear nail polish (Long & Clements, 1934). Each peel was mounted on a slide with 70% glycerol and imaged at multiple focal depths using a Nikon Eclipse E800 microscope (Nikon, Tokyo, Japan) at 400 \times magnification. Stomata were counted in one to three random fields of view (0.071 mm²) per epidermal peel ($n = 186$). Ellipses were fit to ten haphazardly selected stomata per field of view in NIS Elements software (Nikon, Tokyo, Japan), from which guard cell lengths were calculated ($n = 560$).

2.3 | Statistical analysis

We used mixed-effects linear models to determine whether and how strongly CO₂, N or their interaction (all fixed effects) influenced leaf functional traits. A random effect for block and random interaction terms for block \times CO₂ and block \times N were included in all models to account for spatial variability in growth conditions and multiple measurements occurring within treated subplots (i.e. chambers) within blocks. Additional effects for leaf side (fixed), plant identity (random), as well as month, year and their interaction (all random) were included for datasets containing measurements made at multiple levels of these factors. We used multimodel inference to quantify the influence of fixed effects on each response variable while accounting for model selection uncertainty (Grueber, Nakagawa, Laws, & Jamieson, 2011). This approach yields coefficients (denoted β) for each effect that, when derived as described below, are proportional to effect sizes; the approach does not rely on binary indicators of significance (i.e. p values). Coefficients were estimated for each full model and its hierarchically complete subsidiary models; model averaging was used to determine the mean and standard error of coefficients across models. As all fixed effects were binary, they were centred to ± 0.5 such that the magnitude and sign of coefficients would represent effect sizes and directions (Gelman, 2008). Maximum-likelihood estimation was used to fit models; coefficient averages were computed over all models with $\Delta AIC_c < 6$. For the purposes of averaging, coefficients were assigned values of zero for models in which they did not occur. Residual normality was assessed using quantile–quantile plots and was deemed acceptable in all cases.

Linear regression models were used to determine how strongly A_{sat} stimulation, defined as the percentage increase of a parameter mean under treatment conditions relative to the control, and monthly mean salinity were associated over the 3 years of the study. Separate models were fit for each of the three treatment groups ($n = 9$ each). Because it was not clear whether low A_{sat} stimulation values in June 2011 were observed because treatments had only been in place for a month or if low salinity was responsible, we repeated the regression analysis without the data from that month.

Multivariate trait responses to CO₂ and N treatments were evaluated with principle components analysis (PCA). So that we could use this analysis to determine how morphological and physiological trait categories responded to eCO₂ or N, we did not include traits whose membership in these categories was ambiguous (namely *CCI* and stomatal characteristics). Trait means at the chamber level were used in the PCA and eigenvalues were determined from a correlation matrix. All data analyses were carried out using R 3.3.1 (R Foundation for Statistical Computing, Vienna, Austria) with functions from the *lme4* and *MuMIn* libraries used for mixed-effects modelling and multimodel inference, respectively.

2.4 | Simulation model

We evaluated the individual and combined effects of morphological and physiological responses to eCO₂ and N using PhraGPP, a simulation model of annual carbon assimilation by *P. australis* under the global change conditions investigated at GREW (introduced in Caplan et al., 2015 and described in Appendix S2). PhraGPP combines a subset of the leaf-level trait data outlined above together with additional measurements from the field study (e.g. internode distances) and empirical data drawn from other studies of *P. australis* (Table 1). Each run simulates a monotypic stand growing at a specified spatial density and whose leaf and stem properties take on characteristics from one of the four treatment combinations at GREW. Using hourly data on PFD and ambient temperature as forcing variables, it determines carbon gain by the *P. australis* canopy as a stand grows at daily intervals through the growing season. Factors like leaf mortality, light attenuation within the stand and variation in photosynthetic rates through the canopy are accounted for but do not vary with environmental conditions (Table 1; Appendix S2). For the purposes of this study, we modified the original model to allow treatments to be assigned to morphological and physiological characteristics independently.

We ran four sets of simulations, all of which had a stand density of 100 stems/m²; this is a typical density for *P. australis* in North America (Mozdzer et al., 2013). In the first set, morphological and physiological characteristics simultaneously took on values from each of the three treatments (eCO₂, N and eCO₂ + N; these are denoted “full” runs). Next, we ran a set in which all characteristics took on values measured under control conditions (denoted “control” runs). Subsequently, we ran simulations in which only morphological characteristics or only physiological characteristics took on values corresponding to the three global change treatments; values

TABLE 1 Summary of PhraGPP, a simulation model of carbon gain by monotypic *Phragmites australis* stands

Component	Property	Determination	Details
Stand	Treatment	Established at outset	Four levels: Ctrl, eCO ₂ , N, eCO ₂ + N
	Density	Established at outset	100 stems/m ²
Stem	Height	Random draw from curve set, treatment	Logistic equation fit to weekly measurements from 113 plants (Figure S2)
	Number of leaves	Stem height	Linear regression using data from 24 plants (Figure S3)
Leaf	Rank	Numbered sequentially	Apical leaf = 1
	Vertical position	Leaf rank, stem height, treatment	Spline functions fit to data from 24 plants (Figure S4)
	Area	Leaf rank, treatment	Means of data by leaf rank from 36 plants (Figure S5)
	Living/dead	Leaf age	Constant life span assumed (75 days)
Canopy layer	Total leaf area	Leaf area, vertical position	All leaves included (= LAI)
	Living leaf area	Leaf area, living/dead	Live leaves only
	PPFD fraction	Total leaf area	Beer's law using coefficient for <i>P. australis</i>
	Positional correction	Treatment	Quadratic function applied to A _{net} and R _d (Figure S7)
Carbon assimilation	Photosynthesis rate	Treatment, month, PPFD time series	A _{net} from light response curves based on 3 plants per chamber per month (Figure S6)
	Respiration rate	Treatment, month	R _d from light response curves used at all PPFD
	Temperature correction	Q ₁₀ coefficient, temperature time series	Separate Q ₁₀ values for photosynthesis and respiration

Determination indicates dependencies among model properties and other factors used in calculations; *Details* includes the datasets, functions and other information used. Appendix S2 in the Supporting Information contains a comprehensive description of PhraGPP.

TABLE 2 Means and standard errors for physiological variables

Treatment	A _{sat} (μmol m ⁻² s ⁻¹)	R _d (μmol m ⁻² s ⁻¹)	φ (μmol/μmol)	LCP (μmol m ⁻² s ⁻¹)	g _s (mol m ⁻² s ⁻¹)	E (mmol m ⁻² s ⁻¹)	WUE _i (μmol/mmol)
Control	18.47 ± 0.46	1.04 ± 0.04	0.049 ± 0.001	21.78 ± 0.74	0.27 ± 0.01	3.85 ± 0.17	4.59 ± 0.17
eCO ₂	25.29 ± 0.67	0.68 ± 0.03	0.055 ± 0.001	12.53 ± 0.58	0.18 ± 0.01	2.87 ± 0.14	8.71 ± 0.29
N	21.70 ± 0.62	1.24 ± 0.05	0.046 ± 0.001	27.93 ± 1.24	0.30 ± 0.02	4.27 ± 0.19	5.07 ± 0.24
eCO ₂ + N	28.87 ± 0.70	0.82 ± 0.04	0.056 ± 0.001	15.01 ± 0.71	0.22 ± 0.01	3.26 ± 0.14	8.54 ± 0.27

A_{sat}, light-saturated photosynthesis; R_d, dark respiration; φ, quantum efficiency; LCP, light compensation point; g_s, stomatal conductance to water; E, transpiration; WUE_i, water use efficiency.

Statistical evaluations of these variables are presented in Table S1.

measured under control conditions were used for all other characteristics. These are denoted “morphology-only” and “physiology-only,” respectively. We replicated each type of simulation 20 times to account for random selection of height growth curves at the outset of each run. Means of annual data across replicate runs were used to determine the relative effect of each treatment on morphology, physiology or both on annual carbon assimilation rates (GPP).

3 | RESULTS

3.1 | Individual trait responses

Both eCO₂ and N affected photosynthetic light response parameters in *P. australis* (Table 2 and Table S1). In the absence of global change treatments, mean (± SE) A_{sat} over all measurement periods

was 18.5 ± 0.5 μmol m⁻² s⁻¹. Under eCO₂ and N, A_{sat} was stimulated by 37% (β = 0.540) and 17% (β = 0.254; Figure 1), respectively. Moreover, the effects of eCO₂ and N on A_{sat} were approximately additive (i.e. neither synergistic nor antagonistic), reaching 56% under eCO₂ + N (28.9 ± 0.7 μmol m⁻² s⁻¹). The standardized coefficient for the CO₂ × N interaction was correspondingly small (β = 0.010).

R_d and LCP were also influenced by both eCO₂ and N (Table 2). eCO₂ decreased R_d and LCP relative to the control (β = -0.494 and -0.590, respectively; Table S1), whereas N enrichment increased means for both parameters (β = 0.219 and 0.238, respectively). The combined effect of eCO₂ + N yielded mean R_d and LCP values between those measured under eCO₂ and under control conditions (Table 2). Quantum efficiency (φ) was primarily affected by the CO₂ concentration (β = 0.351), increasing by 12% under eCO₂.

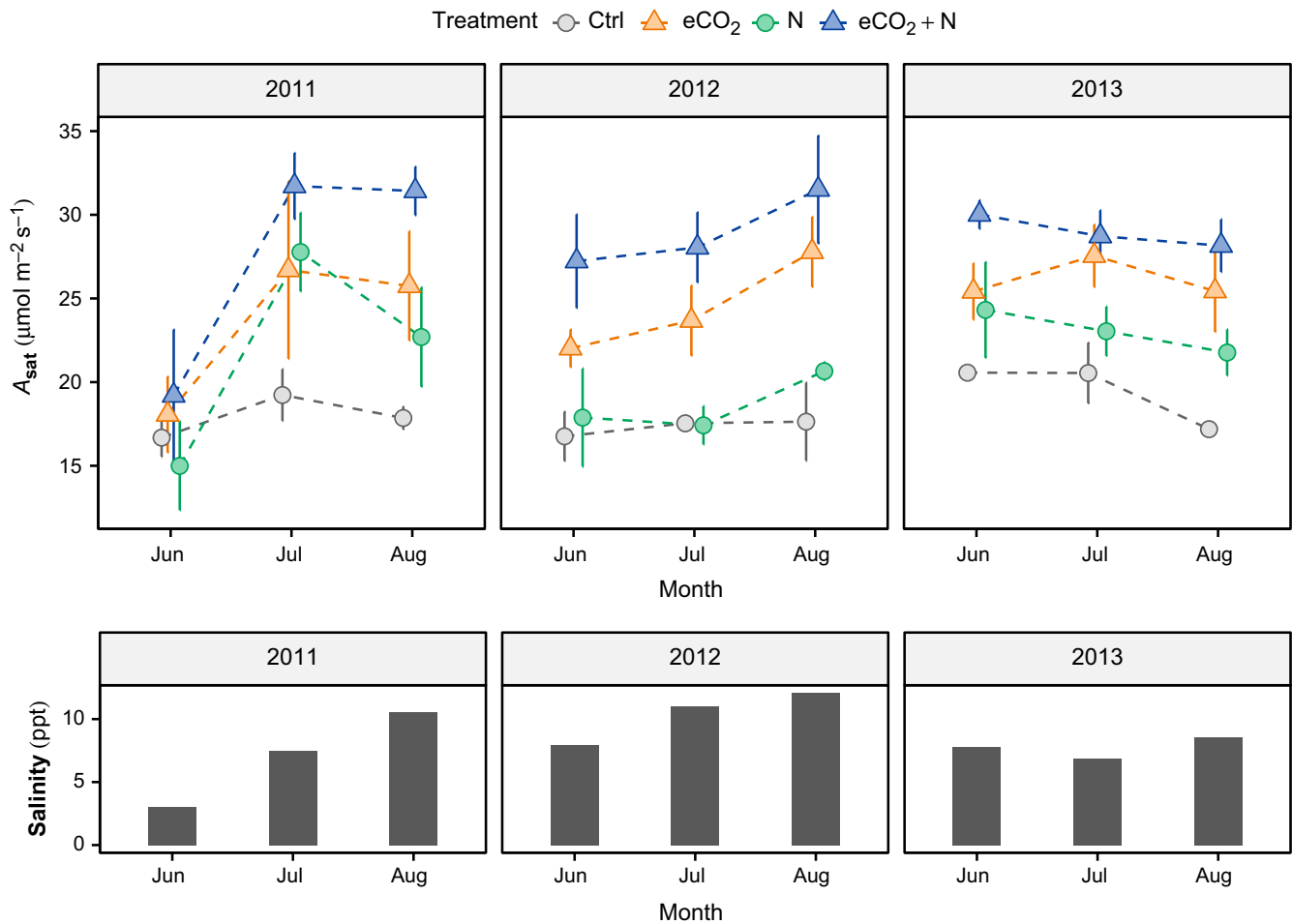


FIGURE 1 (Top) Monthly rates of light-saturated photosynthesis (A_{sat}) over 3 years by *Phragmites australis*. Treatments include exposure to elevated CO_2 ($e\text{CO}_2$), nitrogen (N), both $e\text{CO}_2$ and N ($e\text{CO}_2 + \text{N}$), and the control (Ctrl). Values represent chamber-level means (\pm SE, as computed across chambers), derived from three replicate light curves per chamber per month. (Bottom) Mean salinity on the dates of ecophysiological data collection

Elevated CO_2 decreased *P. australis*' E and g_s rates by 25% ($\beta = -0.351$) and 33% ($\beta = -0.376$) relative to control conditions, respectively, whereas N enrichment increased E and g_s by 11% in both cases ($\beta = 0.125$ and 0.118 , respectively; Table 2 and Table S1). Moreover, WUE_i nearly doubled under elevated vs. ambient CO_2 ($\beta = 0.689$). Although both A_{sat} and E contributed to this increase in WUE_i , the magnitudes of stimulation effects indicate that WUE_i was more strongly influenced by an increase in carbon fixation than by a reduction in water loss (Figure S1).

A_{sat} exhibited a moderate amount of temporal variation, and this corresponded modestly to variation in tide water salinity for plants grown at ambient CO_2 (Figure 1). In addition, we found a strong relationship between salinity and the size of the relative increase in A_{sat} under $e\text{CO}_2$ (Figure 2). Linear regressions of these variables yielded R^2 values of .70 for $e\text{CO}_2$ ($\beta = 0.839$) and .78 for $e\text{CO}_2 + \text{N}$ ($\beta = 0.885$). Without data for June 2011, salinity remained a strong predictor of A_{sat} stimulation in the $e\text{CO}_2 + \text{N}$ group ($R^2 = .53$, $\beta = 0.732$), although the relationship was less strong in the $e\text{CO}_2$ group ($R^2 = .43$, $\beta = 0.657$).

N enrichment had stronger effects on *P. australis* morphology than did elevated CO_2 . On average, stems grew 26.8% taller in response to N ($\beta = 0.257$) but 9.7% taller in response to $e\text{CO}_2$ ($\beta = 0.064$; Figure 3a; Table S1). Similarly, mean leaf area was 46.3% greater under N than the control ($\beta = 0.441$) and only 10.1% greater under elevated vs. ambient CO_2 ($\beta = 0.118$; Figure 3b). Although we did not find evidence for an interaction between N and CO_2 with respect to stem height ($\beta = -0.011$), the increase in leaf area due to N enrichment was approximately halved under elevated vs. ambient CO_2 ($\beta = -0.233$). N induced proportional increases in leaf width and length ($\beta = 0.002$ for the width: length ratio), although leaves became more narrow under $e\text{CO}_2$ ($\beta = 0.148$). SLA rose by 4.7% under $e\text{CO}_2$ vs. control conditions ($\beta = 0.116$) but was unaffected by N ($\beta = -0.003$; Figure 3c). In addition to having strong effects on leaf size, N nearly doubled CCI (86.4% increase, $\beta = 0.741$; Figure 3d). However, this effect was reduced to 53.5% under $e\text{CO}_2$ ($\beta = -0.341$ for the $\text{CO}_2 \times \text{N}$ interaction) and $e\text{CO}_2$ alone yielded no measurable change from control conditions (Figure 3b).

Stomatal characteristics were also altered by global change treatments. Data presented strong evidence that guard cell length

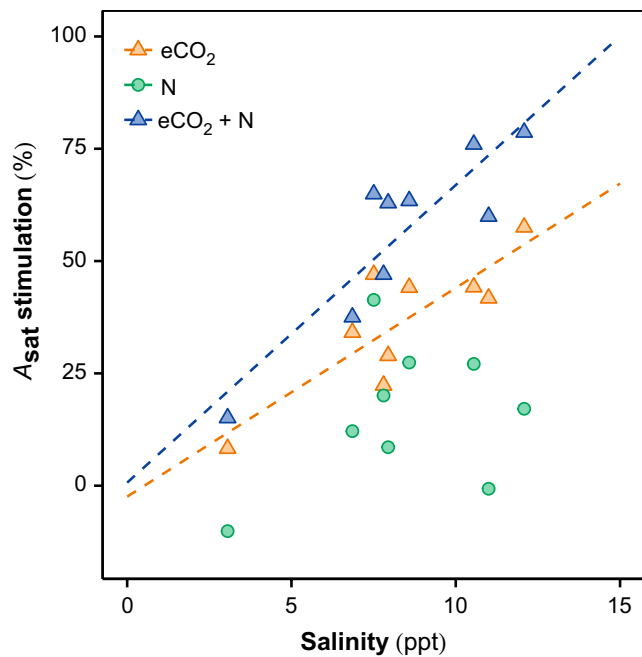


FIGURE 2 Relationship between tide water salinity and the stimulation to light-saturated photosynthetic rate (A_{sat}) by experimental treatments over the nine measurement periods of the study. Stimulation was computed as the per cent change in A_{sat} for treatment vs. control conditions (see Figure 1 for abbreviations); monthly means across replicate chambers are shown

increased with N enrichment ($\beta = 0.255$) and were longer on the adaxial side of leaves ($\beta = 0.121$; Figure 3e). In contrast, stomatal density increased under $e\text{CO}_2$ ($\beta = 0.183$; Figure 3f). The mean adaxial: abaxial ratio of stomatal density was 0.88 ($\beta = 0.089$ for the effect of side).

3.2 | Multivariate trait comparison

PCA illustrated clear shifts in physiological and morphological traits for *P. australis* in response to global change treatments (Figure 4). Axis 1 explained 45% of the variation in trait expression and corresponded to growth under ambient vs. elevated CO_2 ; the ambient CO_2 group had negative values on axis 1, whereas the $e\text{CO}_2$ group had positive values. Axis 2 explained the next 26% of the variation in trait expression and corresponded to growth under ambient (negative values) vs. enriched N (positive values). Most of the traits that corresponded more closely to CO_2 level than N level were physiological (R_d , g_s , WUE_i , and ϕ). In contrast, the subset of traits corresponding to N level were morphological (leaf area and stem height). Notable exceptions were A_{sat} , which we considered physiological but increased with $e\text{CO}_2$ and N, as well as SLA and leaf width: length ratio, which we considered morphological but varied with the CO_2 level.

3.3 | Stand-level responses

Full simulations (representing combined morphological and physiological responses) yielded similar stand-level carbon assimilation rates (GPP) under $e\text{CO}_2$ and N (Figure 5). GPP was 2.32 ± 0.04

and $2.22 \pm 0.02 \text{ kg C m}^{-2} \text{ year}^{-1}$ ($M \pm SD$) under these treatments, representing 44 and 37% increases over the mean for the control ($1.62 \pm 0.04 \text{ kg C m}^{-2} \text{ year}^{-1}$), respectively. However, $e\text{CO}_2$ alone induced a physiology-only stimulation of 27%, accounting for 62% of the full $e\text{CO}_2$ response, whereas it induced a morphology-only stimulation of 12%, accounting for 27% of the full $e\text{CO}_2$ response. In contrast, N alone induced a physiology-only stimulation of 6%, accounting for only 15% of the full response to N, whereas N induced a morphology-only stimulation of 36%, which was 97% of the full response to N. In other words, almost two-thirds of the GPP response to $e\text{CO}_2$ can be attributed to physiological changes, whereas nearly the entire N response can be explained by changes in morphology. The response to the combined $e\text{CO}_2 + \text{N}$ treatment was a GPP rate of $3.06 \pm 0.05 \text{ kg C m}^{-2} \text{ year}^{-1}$, with physiology-only and morphology-only simulations yielding rates approximately two-thirds of that value, and accounting for 44 and 35% of the $e\text{CO}_2 + \text{N}$ stimulation effect, respectively. Synergistic effects therefore contributed an additional 21% of the GPP stimulation effect under $e\text{CO}_2 + \text{N}$.

4 | DISCUSSION

We found contrasting results between morphological traits and leaf-level physiological traits in response to interacting global change factors. As expected, *P. australis* displayed strong trait responses to both $e\text{CO}_2$ and N in our field experiment, some of which have been observed previously in containerized settings (Caplan et al., 2014; Eller et al., 2014; Mozdzer et al., 2012). However, because this study was based on mature clones grown in a field setting, it provides a more realistic assessment of the magnitude of morphological and physiological responses to these interacting global change factors. We specifically found that leaf-level morphological traits (e.g. leaf area) had stronger responses to N enrichment than did leaf-level physiological traits. In contrast, we found that $e\text{CO}_2$ elicited stronger effects on gas exchange physiology (e.g. A_{sat} , g_s , ϕ and LCP) than on morphology. The divergent but complementary nature of these responses suggests that examining morphological and physiological traits in combination can yield far greater insight into plant responses to interacting global change factors than can focusing on either morphological or physiological traits alone.

4.1 | Responses to elevated CO_2

Elevated CO_2 enhanced the physiological performance of *P. australis* and these effects were further enhanced by increasing salinity. The magnitude of increases in A_{sat} (37% stimulation) and decreases in R_d (35% reduction) that we observed under $e\text{CO}_2$ are on par with those reported from other global change experiments (e.g. Ainsworth & Long, 2005). Our data also lend support to a suggestion that $e\text{CO}_2$ induces stronger responses in gas exchange physiology than in leaf morphology, such that that the responses of morphological traits to $e\text{CO}_2$ do not predict the organismal-level response accurately (Temme et al., 2015).

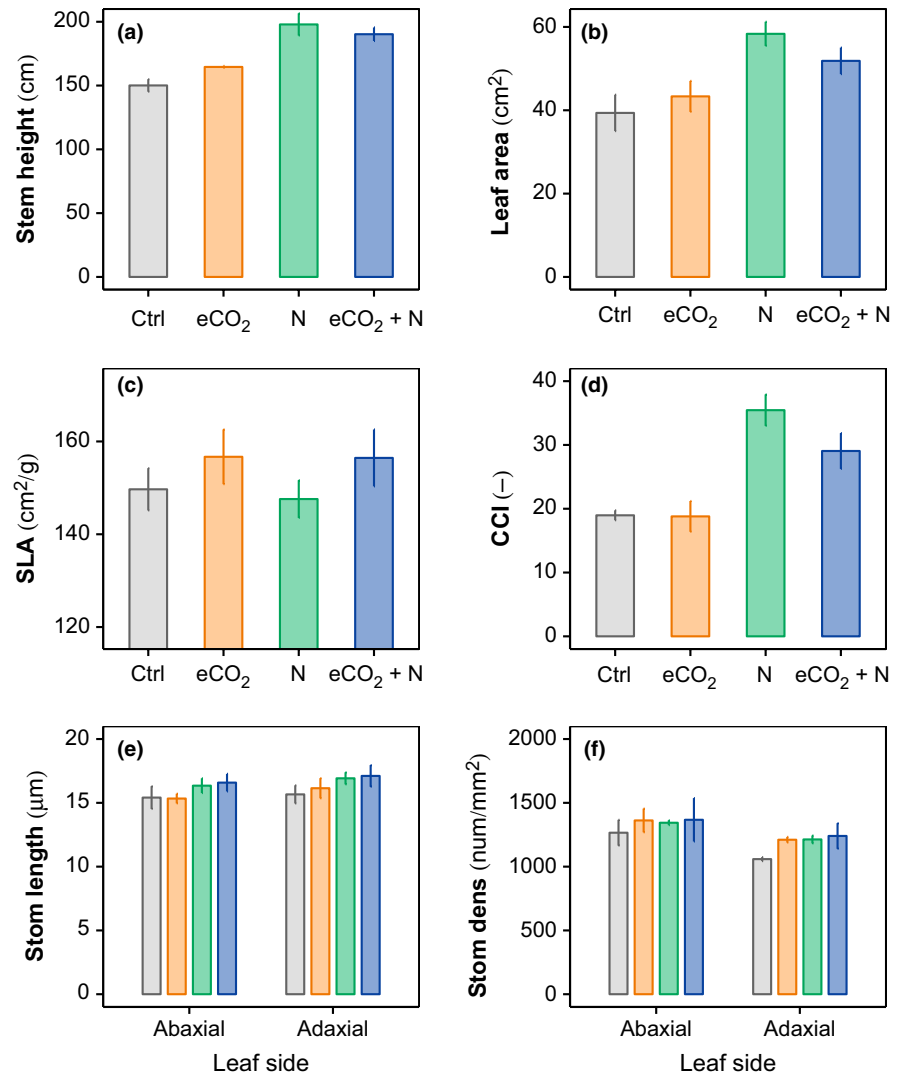


FIGURE 3 Leaf functional traits for *Phragmites australis* plants under experimental conditions. SLA, specific leaf area; CCI, chlorophyll content index; Stom length, stomatal length; Stom dens, stomatal density; see Figure 1 for treatment abbreviations. Bar heights are $M \pm SE$, calculated across replicate chambers

It is likely that the strengthening effect that salinity had on A_{sat} stimulation manifested due to physiological adjustments that altered plant–water relations. As salinity increased under current CO₂ concentrations, changes in osmotic potential, and thus leaf water potential, likely led to stomatal closure and ultimately the observed decline in A_{sat} . In contrast, under elevated CO₂, stronger CO₂ diffusion gradients and increased WUE_i would have mitigated these effects, at least within the salinity range observed (4–18 ppt). Furthermore, it is possible that an enhanced availability of non-structural carbohydrates under elevated CO₂ (Cheng, Moore, & Seemann, 1998) provided an energy subsidy for *P. australis* to mitigate the osmotic stress associated with salinity (Tattini, Gucci, Romani, Baldi, & Everard, 1996).

The approximately linear increase in eCO₂ stimulation that *P. australis* exhibited with increasing salinity over the 3-year period of study (range = 4–18 ppt) was a stronger response than previously described in a native tidal marsh species or in *P. australis* itself. Specifically, prior research on *Schoenoplectus americanus*, the dominant native C₃ species in North American brackish marshes of the Gulf & Atlantic Coasts, as well as at our field site, found that the eCO₂ stimulation effect was lost during high salinity years

(Erickson, Megonigal, Peresta, & Drake, 2007). A previous study of *P. australis* found that eCO₂ alleviated salinity stress (Eller et al., 2014), although this was at a greater salinity level than occurred at our site (20 ppt). Another study of an invasive species found eCO₂ to have no effect on drought responses (Smith et al., 2000), which are physiologically similar to those of salinity. However, it is not clear whether the divergent interactions between salinity and eCO₂ in these studies arose due to differences in biology (e.g. genetics or ontogeny) or environment (e.g. the salinity range), as both differed.

Although plants typically decrease stomatal density and area in response to eCO₂ (Poorter et al., 2012), we found the opposite for *P. australis*. However, our results are not unique, as a number of studies have reported increases (Apel, 1989; Watson-Lazowski et al., 2016; Zhou et al., 2013) or no change (Field, Duckett, Cameron, & Pressel, 2015; Luomala, Laitinen, Sutinen, Kellomaki, & Vapaavuori, 2005; Reid et al., 2003; Tricker et al., 2005) in response to eCO₂. Our data are comparable to previously published data on stomatal size and density in introduced *P. australis* (Hansen, Lambertini, Jampeetong, & Brix, 2007; Saltonstall, 2007), although these studies

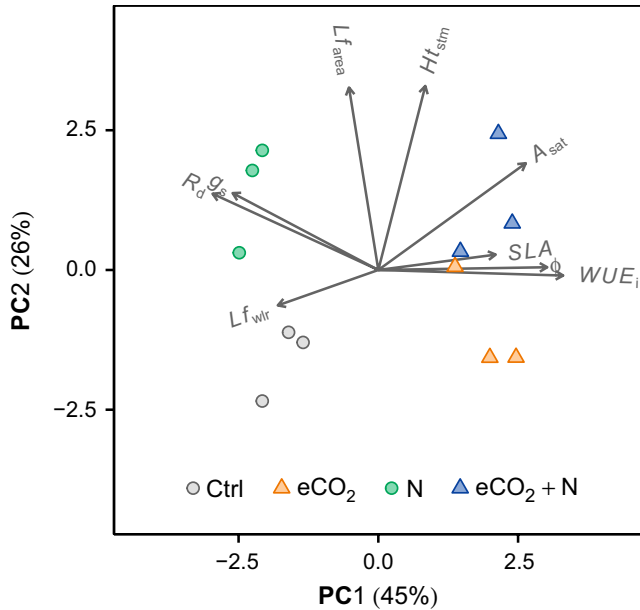


FIGURE 4 Principal components (PC) analysis of plant physiological and morphological traits in response to elevated CO_2 and N treatments. Each point represents a chamber. Abbreviations are defined in Table 2; also, SLA , specific leaf area; Lf_{wlr} , leaf width-to-length ratio

did not evaluate effects of $e\text{CO}_2$. Decreasing stomatal density under $e\text{CO}_2$ is an adaptive strategy to reduce water loss while maintaining carbon fixation (Woodward & Kelly, 1995). Greater stomatal density may have instead allowed for greater CO_2 influx, and thus maintenance of higher photosynthetic rates, under $e\text{CO}_2$. A similar explanation may apply to the increase in stomatal length under N enriched conditions that we observed. If adjustments in stomatal morphology were, in fact, adaptive, changes in stomatal morphology would appear to be another way in which phenotypic plasticity underpins *P. australis*' high productivity response to $e\text{CO}_2$ (Caplan et al., 2015; Mozdzer et al., 2012).

Photosynthetic enhancements under $e\text{CO}_2$ and increasing salinity may promote *P. australis* and potentially alter the abundance of other species in brackish wetlands in the near-future. This possibility is consistent with the finding that the greatest expansion rate of *P. australis* over the past 50 years has occurred in brackish, and not tidal fresh, North American saltmarshes (Chambers et al., 1999). Our study also suggests that global change may facilitate *P. australis* invasion into increasingly saline habitats and that near-future global $e\text{CO}_2$ may alleviate salinity stress from saltwater intrusion associated with sea level rise. Although stronger responses in A_{sat} to $e\text{CO}_2$ with greater salinity are known in obligate halophytes (Ball & Munns, 1992), stimulation of A_{sat} under moderate salinity levels has not been reported in facultative halophytes like *P. australis*. Although potentially coincidence, rates of invasion increased after the 1960s in North America (Saltonstall, 2002), corresponding to the greatest change in global CO_2 concentrations in millennia. Given its strong photosynthetic response to elevated CO_2 , it is possible that recent changes in CO_2 concentrations

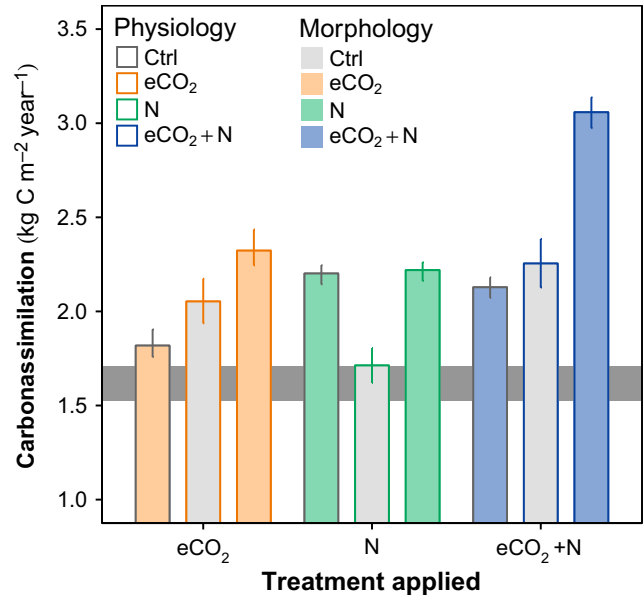


FIGURE 5 Annual carbon assimilation for simulated *Phragmites australis* stands having 100 stems/ m^2 . Bar outline and fill colours correspond to the treatments used for morphological and physiological characteristics, respectively. The grey horizontal band depicts carbon assimilation with all characteristics set to control values. Bar heights show means of 20 replicate runs, with error bars (or grey shading in the control) depicting ranges across replicates

(360–400 ppmv) facilitated the invasion and expansion of *P. australis* in brackish wetlands. Although it is not possible to predict the $e\text{CO}_2$ stimulation response in saline wetlands (>20 ppt) based on our results, a short-term greenhouse experiment indicated that the effects of salinity in the 20 ppt range will be alleviated with elevated CO_2 (Eller et al., 2014).

4.2 | Responses to nitrogen

Nitrogen enrichment induced strong responses in morphology but had relatively small effects on physiology. The 30–50% increase in leaf area with N enrichment ($e\text{CO}_2 + \text{N}$ and N, respectively), when combined with simultaneous increases in plant height, yielded substantially enlarged canopies (Figure 4, Caplan et al., 2015). Although the effect of N enrichment on A_{sat} stimulation (17%) was less than half of that for $e\text{CO}_2$ (37%), these small physiological enhancements, in combination with the substantially enlarged photosynthetic canopies, may explain the high net primary productivity of *P. australis* in the field (Caplan et al., 2015). They may also explain the previously described correlation of *P. australis* invasion with nutrient enrichment facilitated by coastal development (Bertness, Ewanchuk, & Silliman, 2002; King, Deluca, Whigham, & Marra, 2007). As expected, R_d also increased in the N treatment, which can be attributed to increased metabolic activity associated with carbon fixation and N metabolism (Hymus, Snead, Johnson, Hungate, & Drake, 2002).

Although the evidence for a relationship between salinity and A_{sat} stimulation under N enrichment was weak, the smallest A_{sat}

stimulation values occurred in months with the highest salinities in 2012 and 2013 (Figure 2). If real, this would suggest that increasing salinity negatively affects A_{sat} stimulation due to N enrichment. Nevertheless, our data suggest that N enrichment cannot alleviate the negative physiological effects of salinity on A_{sat} , unlike $e\text{CO}_2$. These contrasting responses to salinity merit further study.

Morphological responses to N enrichment are likely to contribute substantially to *P. australis*' invasion. Our findings largely agree with previous studies insofar as they demonstrate that N enrichment enhances *P. australis* growth (Caplan et al., 2015; King et al., 2007). However, the results of this study specifically indicate that rapid carbon gain, and ultimately the invasion itself, can largely be attributed to N enhancing traits contributing to canopy size (e.g. stem height and leaf area). In addition, *P. australis* invasions are not likely to be limited by N availability once established given the lineage's ability to root deeply (Mozdzer, Langley, Mueller, & Megonigal, 2016) and increase N availability by priming the microbial decomposition of organic matter (Bernal, Megonigal, & Mozdzer, 2017).

4.3 | Responses to $e\text{CO}_2$ + N

Our data show that morphological and physiological traits can change in complementary ways to maximize organismal-level productivity. The evidence of $e\text{CO}_2 \times \text{N}$ interactions in leaf area and, to a lesser degree A_{sat} , highlights the interactions that occur between morphology and physiology to optimize productivity under multiple global change factors. Furthermore, our analysis clearly demonstrates that N primarily altered plant morphological traits while $e\text{CO}_2$ primarily altered gas exchange physiology. This interpretation is supported by both our multivariate analysis (Figure 4) and our simulation results (Figure 5). Although A_{sat} was also stimulated by N, it was more strongly stimulated by $e\text{CO}_2$. However, without a concomitant increase in N, restricted leaf areas could severely limit rates of carbon gain.

The complementary responses that *P. australis* has to $e\text{CO}_2$ and N will undoubtedly enhance its growth and invasion under near-future CO_2 conditions. However, enhanced productivity in a future $e\text{CO}_2$ environment may be largely mediated by N availability (Reich et al., 2006), with productivity much greater in wetlands that have greater N inputs. With respect to management, our results suggest that invasions of *P. australis* and other invasive plants may be restricted by limiting N sources to wetlands, such as urban and agricultural runoff. Furthermore, given the additive effects of N (on morphology) and $e\text{CO}_2$ (on physiology), future studies should carefully evaluate the combined influence of these factors on plant productivity, and not rely solely on physiology when predicting responses to global change.

4.4 | Stand-scale response

This analysis highlights the value of considering both physiological and morphological traits when inferring plant responses to global change at the canopy scale. If we had only considered

physiological stimulation, our analysis would have underestimated the N response by >95% and the CO_2 response by nearly 30%, due to complementary changes in morphology in response to both global change factors. Our data also highlight the need for multi-factor global change studies that will allow for realistic projections of primary productivity under near-future environmental conditions. In contrast to a modelling effort that found $e\text{CO}_2$ and temperature induced changes in photosynthetic canopy size to have minor influences on canopy scale metrics (Bagley et al., 2015), our analysis suggests that 30%–90% of gross primary productivity can be attributed to changes in canopy structure, with the greatest effects from N enrichment. Our results also demonstrate that N effects on leaf morphology and canopy structure can have strong effects on canopy-level carbon gain, which is often attributable to changes in LAI (Reich, 2012).

5 | CONCLUSIONS

Our data suggest that changes in morphological traits may have a greater influence on carbon gain than will leaf-level physiology under global change. Also, the results of this field-based analysis of leaf-level traits in response to realistic global change conditions offer several new insights not possible through previous containerized studies: (1) We observed a sustained stimulation of A_{sat} under elevated CO_2 conditions over a 3-year period, which has not been demonstrated by either FACE or growth chamber experiments in our focal species, *P. australis* (Eller et al., 2014; Milla, Cornelissen, Van Logtestijn, Toet, & Aerts, 2006); (2) we found that brackish salinity enhanced the $e\text{CO}_2$ effect on A_{sat} ; previous studies only demonstrated an alleviation of negative salinity effects at greater salinity levels (Eller et al., 2014); (3) we found that N increased both A_{sat} and leaf area, which together help explain the invasion of *P. australis* in N enriched wetlands (Bertness et al., 2002; King et al., 2007); and (4) N enrichment did not enable *P. australis* to overcome effects of salinity on physiological parameters.

Furthermore, our results suggest that care must be taken when evaluating morphological and physiological trait responses to multiple global change factors. Like other studies (Temme et al., 2015), this study shows that CO_2 increases physiological performance. However, our study also demonstrates that, at the stand scale, physiological acclimation to $e\text{CO}_2$ can be overshadowed by morphological plasticity in response to N. We recommend that future studies of trait responses to multiple global change factors evaluate and incorporate both physiological and morphological traits in order to provide a more comprehensive prediction of the response of any species, whether native or invasive, to near-future global change.

ACKNOWLEDGEMENTS

This study was funded by Maryland Sea Grant (SA7528082, SA7528114-WW), the U.S. National Science Foundation's Long Term Research in Environmental Biology Program (DEB-0950080,

DEB-1457100 and DEB-1557009), Bryn Mawr College and the Smithsonian Institution. We thank Patrick Megonigal for contributions to the experimental design and comments on previous versions of this manuscript. We also thank Rachel Hager, Gary Peresta, Andrew Peresta, Blanca Bernal, Lillian Aoki, Jim Duhs, Emily Maroni and Eleanor Durfee for assistance in the field and laboratory.

AUTHORS' CONTRIBUTIONS

T.J.M. designed and initiated the field study; J.S.C. conceived of and wrote the simulation model. Both authors oversaw and contributed to data collection; J.S.C. analysed the data. T.J.M. and J.S.C. developed and wrote the manuscript collaboratively.

CONFLICT OF INTEREST

The authors have no conflict of interests with respect to this research.

DATA ACCESSIBILITY

Data associated with this paper are available through the Dryad Digital Repository <https://doi.org/10.5061/dryad.r98jq6j> (Mozdzer & Caplan, 2018).

ORCID

Thomas J. Mozdzer  <http://orcid.org/0000-0002-1053-0967>

Joshua S. Caplan  <http://orcid.org/0000-0003-4624-2956>

REFERENCES

- Ainsworth, E. A., & Long, S. P. (2005). What have we learned from 15 years of free-air CO₂ enrichment (FACE)? A meta-analytic review of the responses of photosynthesis, canopy. *New Phytologist*, *165*, 351–371.
- Apel, P. (1989). Influence of CO₂ on stomatal numbers. *Biologia Plantarum*, *31*, 72–74. <https://doi.org/10.1007/BF02890681>
- Bagley, J., Rosenthal, D. M., Ruiz-Vera, U. M., Siebers, M. H., Kumar, P., Ort, D. R., & Bernacchi, C. J. (2015). The influence of photosynthetic acclimation to rising CO₂ and warmer temperatures on leaf and canopy photosynthesis models. *Global Biogeochemical Cycles*, *29*, 194–206. <https://doi.org/10.1002/2014GB004848>
- Ball, M. C., & Munns, R. (1992). Plant-responses to salinity under elevated atmospheric concentrations of CO₂. *Australian Journal of Botany*, *40*, 515–525. <https://doi.org/10.1071/BT9920515>
- Bernal, B., Megonigal, J. P., & Mozdzer, T. J. (2017). An invasive wetland grass primes deep soil carbon pools. *Global Change Biology*, *23*, 2104–2116.
- Bertness, M. D., Ewanchuk, P. J., & Silliman, B. R. (2002). Anthropogenic modification of New England salt marsh landscapes. *Proceedings of the National Academy of Sciences of the United States of America*, *99*, 1395–1398. <https://doi.org/10.1073/pnas.022447299>
- Bradley, B. A., Blumenthal, D. M., Wilcove, D. S., & Ziska, L. H. (2010). Predicting plant invasions in an era of global change. *Trends in Ecology & Evolution*, *25*, 310–318. <https://doi.org/10.1016/j.tree.2009.12.003>
- Caplan, J. S., Hager, R. N., Megonigal, J. P., & Mozdzer, T. J. (2015). Global change accelerates carbon assimilation by a wetland ecosystem engineer. *Environmental Research Letters*, *10*, 115006. <https://doi.org/10.1088/1748-9326/10/11/115006>
- Caplan, J. S., Wheaton, C., & Mozdzer, T. J. (2014). Belowground advantages in construction cost facilitate a cryptic plant invasion. *AoB PLANTS*, *6*, plu020. <https://doi.org/10.1093/aobpla/plu020>
- Chambers, R. M., Meyerson, L. A., & Saltonstall, K. (1999). Expansion of *Phragmites australis* into tidal wetlands of North America. *Aquatic Botany*, *64*, 261–273. [https://doi.org/10.1016/S0304-3770\(99\)00055-8](https://doi.org/10.1016/S0304-3770(99)00055-8)
- Chambers, R. M., Osgood, D. T., Bart, D. J., & Montalto, F. (2003). *Phragmites australis* invasion and expansion in tidal wetlands: Interactions among salinity, sulfide, and hydrology. *Estuaries*, *26*, 398–406. <https://doi.org/10.1007/BF02823716>
- Cheng, S. H., Moore, B. D., & Seemann, J. R. (1998). Effects of short- and long-term elevated CO₂ on the expression of ribulose-1,5-bisphosphate carboxylase/oxygenase genes and carbohydrate accumulation in leaves of *Arabidopsis thaliana* (L) Heynh. *Plant Physiology*, *116*, 715–723. <https://doi.org/10.1104/pp.116.2.715>
- Davidson, A. M., Jennions, M., & Nicotra, A. B. (2011). Do invasive species show higher phenotypic plasticity than native species and, if so, is it adaptive? A meta-analysis. *Ecology Letters*, *14*, 419–431. <https://doi.org/10.1111/j.1461-0248.2011.01596.x>
- Drake, B. G. (2014). Rising sea level, temperature, and precipitation impact plant and ecosystem responses to elevated CO₂ on a Chesapeake Bay wetland: Review of a 28-year study. *Global Change Biology*, *20*, 3329–3343. <https://doi.org/10.1111/gcb.12631>
- Drake, B. G., Leadley, P. W., Arp, W. J., Nassiry, D., & Curtis, P. S. (1989). An open top chamber for field studies of elevated atmospheric CO₂ concentration on saltmarsh vegetation. *Functional Ecology*, *3*, 363–371. <https://doi.org/10.2307/2389377>
- Dukes, J. S. (2000). Will the rising atmospheric CO₂ concentration affect biological invaders? In H. A. Mooney, & R. J. Hobbs (Eds.), *Invasive species in a changing world* (pp. 95–113). Washington, DC: Island Press.
- Eller, F., Lambertini, C., Nguyen, L. X., & Brix, H. (2014). Increased invasive potential of non-native *Phragmites australis*: Elevated CO₂ and temperature alleviate salinity effects on photosynthesis and growth. *Global Change Biology*, *20*, 531–543. <https://doi.org/10.1111/gcb.12346>
- Eller, F., Skalova, H., Caplan, J. S., Bhattarai, G. P., Burger, M. K., Cronin, J. T., ... Brix, H. (2017). Cosmopolitan species as models for ecophysiological responses to global change: The common reed *Phragmites australis*. *Frontiers in Plant Science*, *8*, 1833. <https://doi.org/10.3389/fpls.2017.01833>
- Erickson, J. E., Megonigal, J. P., Peresta, G., & Drake, B. G. (2007). Salinity and sea level mediate elevated CO₂ effects on C₃-C₄ plant interactions and tissue nitrogen in a Chesapeake Bay tidal wetland. *Global Change Biology*, *13*, 202–215. <https://doi.org/10.1111/j.1365-2486.2006.01285.x>
- Field, K. J., Duckett, J. G., Cameron, D. D., & Pressel, S. (2015). Stomatal density and aperture in non-vascular land plants are non-responsive to above-ambient atmospheric CO₂ concentrations. *Annals of Botany*, *115*, 915–922. <https://doi.org/10.1093/aob/mcv021>
- Gelman, A. (2008). Scaling regression inputs by dividing by two standard deviations. *Statistics in Medicine*, *27*, 2865–2873. [https://doi.org/10.1002/\(ISSN\)1097-0258](https://doi.org/10.1002/(ISSN)1097-0258)
- Gonzalez, A. L., Kominoski, J. S., Danger, M., Ishida, S., Iwai, N., & Rubach, A. (2010). Can ecological stoichiometry help explain patterns of biological invasions? *Oikos*, *119*, 779–790. <https://doi.org/10.1111/j.1600-0706.2009.18549.x>

- Grueber, C. E., Nakagawa, S., Laws, R. J., & Jamieson, I. G. (2011). Multimodel inference in ecology and evolution: Challenges and solutions. *Journal of Evolutionary Biology*, 24, 699–711. <https://doi.org/10.1111/j.1420-9101.2010.02210.x>
- Hansen, D. L., Lambertini, C., Jampeetong, A., & Brix, H. (2007). Clone-specific differences in *Phragmites australis*: Effects of ploidy level and geographic origin. *Aquatic Botany*, 86, 269–279. <https://doi.org/10.1016/j.aquabot.2006.11.005>
- Hikosaka, K., Anten, N. P. R., Borjigidai, A., Kamiyama, C., Sakai, H., Hasegawa, T., ... Ito, A. (2016). A meta-analysis of leaf nitrogen distribution within plant canopies. *Annals of Botany*, 118, 239–247. <https://doi.org/10.1093/aob/mcw099>
- Hopkinson, C. S., & Giblin, A. E. (2008). Nitrogen dynamics of coastal salt marshes. In D. G. Capone, D. A. Bronk, M. R. Mulholland, & E. J. Carpenter (Eds.), *Nitrogen in the marine environment* (pp. 991–1036). San Diego, CA: Academic Press. <https://doi.org/10.1016/B978-0-12-372522-6.00022-0>
- Hulme, P. E. (2008). Phenotypic plasticity and plant invasions: Is it all Jack? *Functional Ecology*, 22, 3–7.
- Hymus, G. J., Snead, T. G., Johnson, D. P., Hungate, B. A., & Drake, B. G. (2002). Acclimation of photosynthesis and respiration to elevated atmospheric CO₂ in two Scrub Oaks. *Global Change Biology*, 8, 317–328. <https://doi.org/10.1046/j.1354-1013.2001.00472.x>
- Jordan, T. E., & Correll, D. L. (1985). Nutrient chemistry and hydrology of interstitial water in brackish tidal marshes of Chesapeake Bay. *Estuarine Coastal and Shelf Science*, 21, 45–55. [https://doi.org/10.1016/0272-7714\(85\)90005-8](https://doi.org/10.1016/0272-7714(85)90005-8)
- Keller, J. K., Wolf, A. A., Weisenhorn, P. B., Drake, B. G., & Megonigal, J. P. (2009). Elevated CO₂ affects porewater chemistry in a brackish marsh. *Biogeochemistry*, 96, 101–117. <https://doi.org/10.1007/s10533-009-9347-3>
- King, R. S., Deluca, W. V., Whigham, D. F., & Marra, P. P. (2007). Threshold effects of coastal urbanization on *Phragmites australis* (common reed) abundance and foliar nitrogen in Chesapeake Bay. *Estuaries and Coasts*, 30, 469–481. <https://doi.org/10.1007/BF02819393>
- Langley, J. A., Mckee, K. L., Cahoon, D. R., Cherry, J. A., & Megonigal, J. P. (2009). Elevated CO₂ stimulates marsh elevation gain, counterbalancing sea-level rise. *Proceedings of the National Academy of Sciences of the United States of America*, 106, 6182–6186. <https://doi.org/10.1073/pnas.0807695106>
- Long, F. L., & Clements, F. E. (1934). The method of collodion films for stomata. *American Journal of Botany*, 21, 7–17. <https://doi.org/10.1002/j.1537-2197.1934.tb08925.x>
- Luomala, E. M., Laitinen, K., Sutinen, S., Kellomaki, S., & Vapaavuori, E. (2005). Stomatal density, anatomy and nutrient concentrations of Scots pine needles are affected by elevated CO₂ and temperature. *Plant, Cell and Environment*, 28, 733–749. <https://doi.org/10.1111/j.1365-3040.2005.01319.x>
- McCormick, M. K., Kettenring, K. M., Baron, H. M., & Whigham, D. F. (2010). Extent and reproductive mechanisms of *Phragmites australis* spread in brackish wetlands in Chesapeake Bay, Maryland (USA). *Wetlands*, 30, 67–74. <https://doi.org/10.1007/s13157-009-0007-0>
- Meinshausen, M., Smith, S. J., Calvin, K., Daniel, J. S., Kainuma, M. L. T., Lamarque, J.-F., ... Van Vuuren, D. P. P. (2011). The RCP greenhouse gas concentrations and their extensions from 1765 to 2300. *Climatic Change*, 109, 213–241. <https://doi.org/10.1007/s10584-011-0156-z>
- Meyerson, L. A., Cronin, J. T., & Pysek, P. (2016). *Phragmites australis* as a model organism for studying plant invasions. *Biological Invasions*, 18, 2421–2431. <https://doi.org/10.1007/s10530-016-1132-3>
- Milla, R., Cornelissen, J. H. C., Van Logtestijn, R. S. P., Toet, S., & Aerts, R. (2006). Vascular plant responses to elevated CO₂ in a temperate lowland *Sphagnum* peatland. *Plant Ecology*, 182, 13–24. <https://doi.org/10.1007/s11258-005-9028-9>
- Mozdzer, T. J., Brisson, J., & Hazelton, E. L. G. (2013). Physiological ecology and functional traits of North American native and Eurasian introduced *Phragmites australis* lineages. *AoB PLANTS*, 5, plt048. <https://doi.org/10.1093/aobpla/plt048>
- Mozdzer, T. J., & Caplan, J. S. (2018). Data from: Complementary responses of morphology and physiology enhance the stand-scale production of a model invasive species under elevated CO₂ and nitrogen. *Dryad Digital Repository*, <https://doi.org/10.5061/dryad.r98jq6j>
- Mozdzer, T. J., Langley, J. A., Mueller, P., & Megonigal, J. P. (2016). Deep rooting and global change facilitate spread of invasive grass. *Biological Invasions*, 18, 2619–2631.
- Mozdzer, T. J., & Megonigal, J. P. (2012). Jack-and-master trait responses to elevated CO₂ and N: A comparison of native and introduced *Phragmites australis*. *PLoS ONE*, 7, e42794. <https://doi.org/10.1371/journal.pone.0042794>
- Packer, J. G., Meyerson, A., Richardson, D. M., Brundu, G., Allen, W. J., Bhattarai, G. P., ... Pysek, P. (2017). Global networks for invasion science: Benefits, challenges and guidelines. *Biological Invasions*, 19, 1081–1096. <https://doi.org/10.1007/s10530-016-1302-3>
- Poorter, H., Fiorani, F., Pieruschka, R., Wojciechowski, T., van Der Putten, W. H., Kleyer, M., ... Postma, J. (2016). Pampered inside, pestered outside? Differences and similarities between plants growing in controlled conditions and in the field. *New Phytologist*, 212, 838–855. <https://doi.org/10.1111/nph.14243>
- Poorter, H., Niklas, K. J., Reich, P. B., Oleksyn, J., Poot, P., & Mommer, L. (2012). Biomass allocation to leaves, stems and roots: Meta-analyses of interspecific variation and environmental control. *New Phytologist*, 193, 30–50. <https://doi.org/10.1111/j.1469-8137.2011.03952.x>
- Priou, J. L., & Chartier, P. (1977). Partitioning of transfer and carboxylation components of intracellular resistance to photosynthetic CO₂ fixation: A critical analysis of the methods used. *Annals of Botany*, 41, 789–800. <https://doi.org/10.1093/oxfordjournals.aob.a085354>
- Reich, P. B. (2012). Key canopy traits drive forest productivity. *Proceedings of the Royal Society B-Biological Sciences*, 279, 2128–2134. <https://doi.org/10.1098/rspb.2011.2270>
- Reich, P. B., Hobbie, S. E., Lee, T., Ellsworth, D. S., West, J. B., Tilman, D., ... Trost, J. (2006). Nitrogen limitation constrains sustainability of ecosystem response to CO₂. *Nature*, 440, 922–925. <https://doi.org/10.1038/nature04486>
- Reid, C. D., Maherali, H., Johnson, H. B., Smith, S. D., Wullschlegel, S. D., & Jackson, R. B. (2003). On the relationship between stomatal characters and atmospheric CO₂. *Geophysical Research Letters*, 30, <https://doi.org/10.1029/2003GL017775>
- Richards, C. L., Bossdorf, O., Muth, N. Z., Gurevitch, J., & Pigliucci, M. (2006). Jack of all trades, master of some? On the role of phenotypic plasticity in plant invasions. *Ecology Letters*, 9, 981–993. <https://doi.org/10.1111/j.1461-0248.2006.00950.x>
- Saltonstall, K. (2002). Cryptic invasion by a non-native genotype of the common reed, *Phragmites australis*, into North America. *Proceedings of the National Academy of Sciences of the United States of America*, 99, 2445–2449. <https://doi.org/10.1073/pnas.032477999>
- Saltonstall, K. (2007). Comparison of morphological variation indicative of ploidy level in *Phragmites australis* (Poaceae) from eastern North America. *Rhodora*, 109, 415–429. [https://doi.org/10.3119/0035-4902\(2007\)109\[415:COMVIO\]2.0.CO;2](https://doi.org/10.3119/0035-4902(2007)109[415:COMVIO]2.0.CO;2)
- Smith, S. D., Huxman, T. E., Zitzer, S. F., Charlet, T. N., Housman, D. C., Coleman, J. S., ... Nowak, R. S. (2000). Elevated CO₂ increases productivity and invasive species success in an arid ecosystem. *Nature*, 408, 79–82. <https://doi.org/10.1038/35040544>
- Sullivan, L., Wildova, R., Goldberg, D., & Vogel, C. (2010). Growth of three cattail (*Typha*) taxa in response to elevated CO₂. *Plant Ecology*, 207, 121–129. <https://doi.org/10.1007/s11258-009-9658-4>
- Tattini, M., Gucci, R., Romani, A., Baldi, A., & Everard, J. D. (1996). Changes in non-structural carbohydrates in olive (*Olea europaea*) leaves during root zone salinity stress. *Physiologia Plantarum*, 98, 117–124. <https://doi.org/10.1111/j.1399-3054.1996.tb00682.x>

- Temme, A. A., Liu, J. C., Cornwell, W. K., Cornelissen, J. H. C., & Aerts, R. (2015). Winners always win: Growth of a wide range of plant species from low to future high CO₂. *Ecology and Evolution*, 5, 4949–4961. <https://doi.org/10.1002/ece3.1687>
- Thomas, R. B., & Strain, B. R. (1991). Root restriction as a factor in photosynthetic acclimation of cotton seedlings grown in elevated carbon-dioxide. *Plant Physiology*, 96, 627–634. <https://doi.org/10.1104/pp.96.2.627>
- Tricker, P. J., Trewin, H., Kull, O., Clarkson, G. J. J., Eensalu, E., Tallis, M. J., ... Taylor, G. (2005). Stomatal conductance and not stomatal density determines the long-term reduction in leaf transpiration of poplar in elevated CO₂. *Oecologia*, 143, 652–660. <https://doi.org/10.1007/s00442-005-0025-4>
- Watson-Lazowski, A., Lin, Y. A., Miglietta, F., Edwards, R. J., Chapman, M. A., & Taylor, G. (2016). Plant adaptation or acclimation to rising CO₂? Insight from first multigenerational RNA-Seq transcriptome. *Global Change Biology*, 22, 3760–3773. <https://doi.org/10.1111/gcb.13322>
- Way, D. A., Oren, R., & Kroner, Y. (2015). The space-time continuum: The effects of elevated CO₂ and temperature on trees and the importance of scaling. *Plant, Cell and Environment*, 38, 991–1007. <https://doi.org/10.1111/pce.12527>
- Woodward, F. I., & Kelly, C. K. (1995). The influence of CO₂ concentration on stomatal density. *New Phytologist*, 131, 311–327. <https://doi.org/10.1111/j.1469-8137.1995.tb03067.x>
- Zhou, Y. M., Jiang, X. J., Schaub, M., Wang, X. J., Han, J. Q., Han, S. J., & Li, M. H. (2013). Ten-year exposure to elevated CO₂ increases stomatal number of *Pinus koraiensis* and *P. sylvestrifomis* needles. *European Journal of Forest Research*, 132, 899–908. <https://doi.org/10.1007/s10342-013-0728-8>

SUPPORTING INFORMATION

Additional supporting information may be found online in the Supporting Information section at the end of the article.

How to cite this article: Mozdzer TJ, Caplan JS.

Complementary responses of morphology and physiology enhance the stand-scale production of a model invasive species under elevated CO₂ and nitrogen. *Funct Ecol*. 2018;32:1784–1796. <https://doi.org/10.1111/1365-2435.13106>